PADEU | PADEU **15**, 93 (2005)
ISBN 963 463 557

Identification and Statistical Analysis of Hot Flow Anomalies Using Cluster Multi-Spacecraft Measurements

G. Facskó, K. Kecskeméty, M. Tátrallyay and G. Erdős

KFKI Research Institute for Particle and Nuclear Physics, H-1525 Budapest, Pf. 49, Hungary

E-mail: gfacsko@rmki.kfki.hu

Abstract
Discovered nearly 20 years ago near the Earth's bow shock, the identification and separation of Hot Flow Anomalies (HFAs) from other events is still under debate. We have used the observations of instruments FGM, CIS, and RAPID aboard the four Cluster spacecraft to detect and study these phenomena. The definition and basic features of HFAs (size, direction of tangential discontinuity, electric field, speed of propagation) have been refined, several series of events identified, and a preliminary statistical analysis carried out. After combining data from RAPID and FGM the pitch angle distributions of protons have been calculated. The measured and calculated features of HFA events are confronted with the results of hybrid simulations.
Keywords: *hot flow anomaly, Earth's bow shock, tangential discontinuity*

1 Introduction

ESA's cornerstone mission, CLUSTER has been the most successful magnetosphere project since the satellites were launched in 2000 (Escoubet et al., 1997). The orbits of the four satellites cross the most important parts of the cosmic neighborhood of our planet. Their apogee are upstream of the Earth's bow-shock during spring on the

Northern Hemisphere. This fact, using FGM[1] and CIS[2] instruments allows to detect the relatively rare phenomena called HFA[3] effectively whereas the RAPID energetic particle instrument provides additional information. We processed the measurements of CLUSTER from February 1 through April 8, 2003 and identified nearly 50 HFA events, performed a statistical analysis and refined their basic features. After combining data from the RAPID and FGM instruments pitch angle distributions were calculated using a transformation into the plasma frame (Facskó, 2004). Although no perfect theoretical explanation of HFAs has been made so far, the two hybrid simulations developed seem to reproduce the basic features (Thomas et al., 1991; Lin, 1997, 2002, 2003). The observations of the HFA events found are confronted with the results of these hybrid simulations.

The outline of the paper is as follows: identification, analysis, measured and calculated features of hot flow anomalies are described in Section 2. The comparison of hybrid simulations with observations is presented in Section 3. A summary is given in Section 4

2 Hot Flow Anomalies

No detailed theory has been presented yet which could reproduce all properties of HFAs since they were discovered (Schwartz et al., 1985; Thomsen et al., 1986). Reconnection and ion-beam instability are assumed as energy source of HFAs (Thomas et al., 1991; Lin, 1997). The formation and development of HFAs have been modeled by hybrid simulations (Thomas et al., 1991; Lin, 1997, 2002, 2003). Several features of HFAs were given and their sketch was constructed based upon single spacecraft observations (See: Fig. 1, left panel based on Sibeck et al. (1999); Fig. 1, right panel). The main problem of detecting HFAs is the relatively small size of the volume affected. Satellites must have been at the right place at the right time. The Cluster project has changed this situation revolutionary: the four satellites cover huge space and all satellites have suitable instruments detecting HFA events. Lucek et al. (2004) made the first attempt to use 4-point measurements and examined 3 HFAs within a short time interval when the s/c separation was small (≈100 km).

2.1 Detecting HFAs

Figure 2 depicts a typical hot flow anomaly event and represents criteria for searching. HFAs are the result of the interaction of a tangential discontinuity with the bow-shock of the Earth (Schwartz et al., 2000) or of other object (Øieroset, 2001). We set up the following conditions, which might indicate the presence of a HFA:

[1] **F**lux **G**ate **M**agnetometer
[2] **C**luster **I**on **S**pectrometer
[3] **H**ot **F**low **A**nomaly

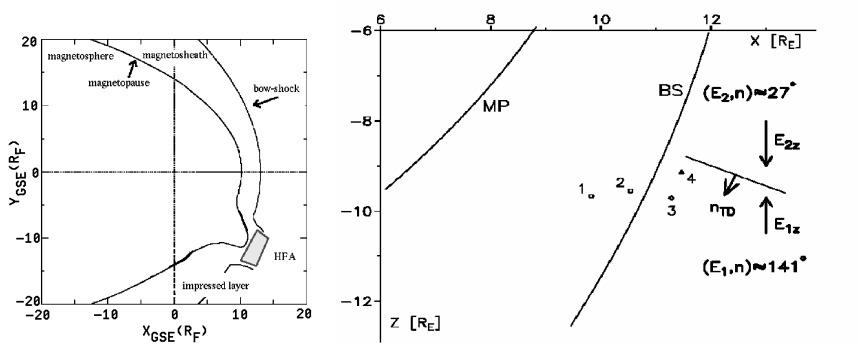

Figure 1: *Left: The supposed structure of HFAs: a tangential discontinuity crosses the bow-shock and they form a hot, tenuous diamagnetic cavity. HFAs seem to be a bulge on both bow-shock and magnetopause. Right: Sketch of the HFA event on February 16, 2003. The normal vector of the tangential discontinuity, the direction of the electric field and the location of the bow-shock and the magnetopause are calculated and plotted.*

- Behavior of the magnetic field, measurements of FGM (Fig. 2, 2nd panel):
  - HFAs appear as a bulge on the bow-shock so one should search them upstream of the shock. That means that the magnitude of the magnetic field has to be near the average interplanetary value.
  - The event begins when the magnitude of the magnetic field drops.
  - FGM observes fast fluctuations in the magnitude of the field and its direction turns around.
  - After the HFA B reaches its value prior to the event.
- Behavior of the solar wind, measurements of CIS HIA[4]:
  - The solar wind slows down, its flow direction might turn back (Fig. 2, 3rd panel).
  - The plasma temperature increases up to several 10 MK (Fig. 2, 4th panel).
  - The plasma density decreases (Fig. 2, 5th panel).
- The fluxes of energetic particles usually increase in the four lower energy channels of RAPID but not always. One can obtain an angular resolution of the

[4]**H**ot **I**on **A**nalyser

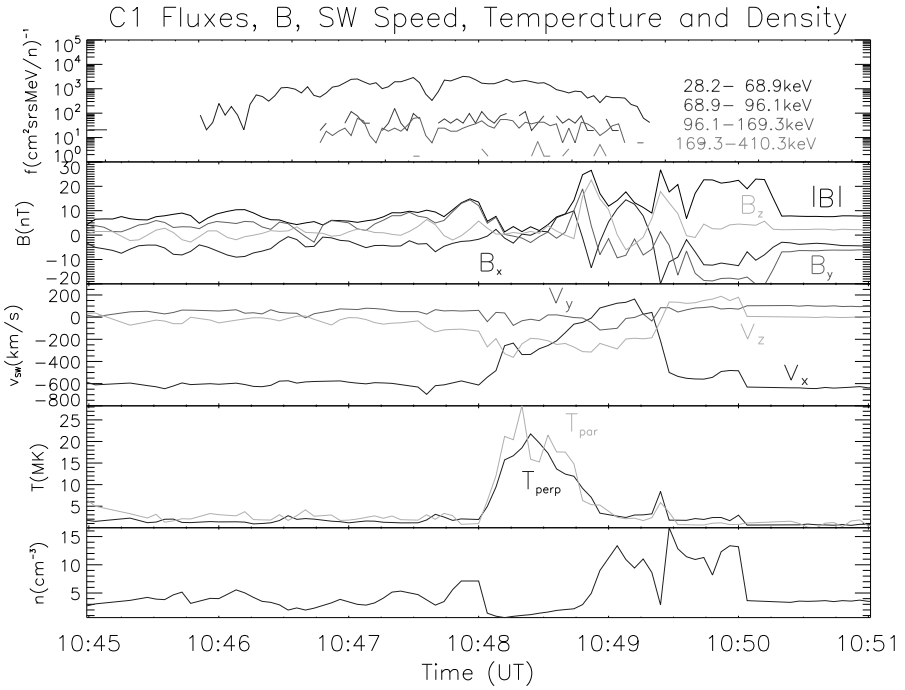

Figure 2: *The first HFA event, detected at 10:45-10:50 UT, on February 16, 2003. Top panel: proton fluxes in four energy channels measured by RAPID aboard Cluster-1. 2nd panel: components and absolute value of magnetic field. 3rd, 4th and 5th panels: components of the solar wind speed, parallel and perpendicular temperature, and the particle density of the solar wind.*

particle fluxes (16×12pixel) and calculate pitch angle distributions by combining data from the RAPID and FGM instruments (Fig. 2, 1st panel).

- The right direction of electric field seems to be the most important condition. The E field focuses particles towards the tangential discontinuity so that its direction should point towards it on both sides.

We found about fifty candidates of HFA events after processing Cluster measurements from February to April, 2003 when the separation between the 4 s/c was of the order of 10,000 km.

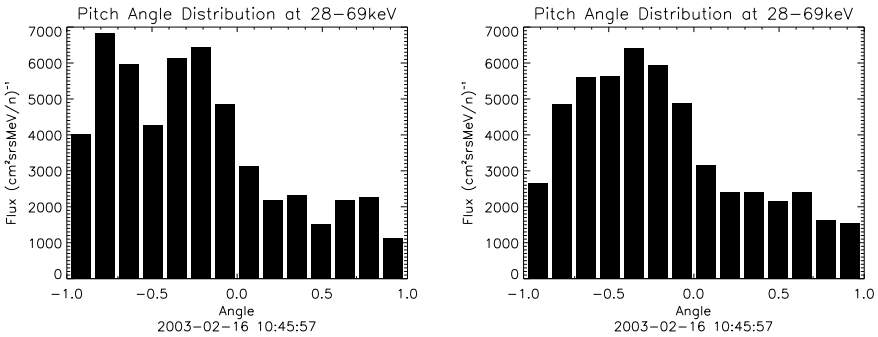

Figure 3: *Pitch angle distribution of 28-69 keV protons during the HFA event at 10:45-10:50 UT on February 16, 2003. Left: PAD calculated with 128s averaged magnetic field. Right: Average of four PADs calculated with 32s averaged magnetic field.*

2.2 Pitch Angle Distributions

After combining data from the RAPID and FGM instruments pitch angle distributions (PADs) of the lowest energy (28-69 keV) protons were calculated for the HFA event 10:45-50 UT on February 16, 2003. The sensitivities of the IIMS[5] detector heads have significantly decreased since launch, we have corrected for this, then the fluxes were transformed to the frame of solar wind using actual CIS solar wind speed measurements and spectral slope from RAPID (Compton-Getting effect). Unfortunately, the cycle of collecting a full directional distribution was about 128 s, 32 times the spin period of Cluster. The simplest choice is to average the magnetic field direction over this period and then compute the pitch angles accordingly. However, the direction of B usually changes much more rapidly than that (Fig. 3, left panel). In lack of higher resolution information one can try to average the B directions over shorter periods (say 32 s instead of 128 s) and assume that the measured directional distribution does not change significantly over that time. Then one has 4 different PADs for the 128 s period which can be averaged. We carried out the two procedures, divided the $[-1, 1]$ interval of $\cos\alpha$ into subintervals, added the fluxes and counted the number of points of those points which have suitable pitch angle. We calculated the average flux of subintervals and then we plotted both pitch angle distributions (Fig. 3, right panel).

2.3 Statistical Aspects

As a result of a survey of the period between February 15 and April 20 about 50 events were found that fulfilled out requirements for HFA events. Most of them were seen by

[5]**I**maging **I**on **M**ass **S**pectrometer

all Cluster satellites while some of them only by one or two spacecraft. Summarizing their general parameters we found that x component of the solar wind decreased usually by 200-400 km/s (in 3 extreme cases the plasma speed became antisolar but in some other events the drop was not more than 50 km/s). V_z changed significantly in all events because they were observed at higher latitudes. The proton density as measured by the HIA sensor of CIS dropped to or below $1/cm^3$ in most cases (about 80% of all), and the parallel proton temperature increased to more than 10 MK in nearly all events. The magnetic field in the cavity was usually below 3 nT. The differences observed in parameters at different spacecraft are generally small. The energetic proton signatures associated with these events were highly variable: in about 20 cases the 28-69 keV proton flux peak exceeded 1000 p/(cm^2 s sr keV) for at least one spacecraft. The particle events usually exhibited smooth profiles starting before and ending after the plasma and magnetic field signatures.

The events were not randomly distributed in time, many of them appeared in sequences within about 1-2 hours (4 on 16 February, 4 on 17 February, 3 on 7 March, 7 on 17 March, 5 on 19 March, 7 on 21 March, and 4 on 24 March). This may indicate preferable conditions rather than grouping of discontinuities. In most cases the solar wind velocity and dynamic pressure was very high compressing the magnetopause and the bow shock.

3 Hybrid Simulations

The hybrid simulation of the plasma is a combination of a full particle approach and a fluid approach. It models the plasma dynamics by treating the ions as particles and the electrons as a charge-neutralizing fluid. Many kinds of hybrid code exist; ions can be treated as macroparticles, the electron fluid might be massless or can have finite mass, the network of the simulation might be two or three dimensional, Cartesian or curvilinear, adaptive or not adaptive. Thomas et al. (1991) and Lin (1997, 2002, 2003) have developed hybrid HFA simulation codes. We studied, checked and compared their result with our observations.

3.1 Results

The hybrid code developed by Thomas et al. (1991) studied the close surroundings of HFAs. The tangential discontinuity intersected the bow shock perpendicularly and they sliced the simulation space and made magnetic field, temperature and particle density diagrams. The form of both magnetic field and particle density diagrams is similar: two small peaks appear at the beginning and the end of the event and both quantities decrease in the middle of the event. The temperature increases in his model.

The other hybrid code developed by Lin (1997, 2002, 2003) uses larger simulation space. A solid target is inserted into superalvénic flow and bow shock form. The flow is

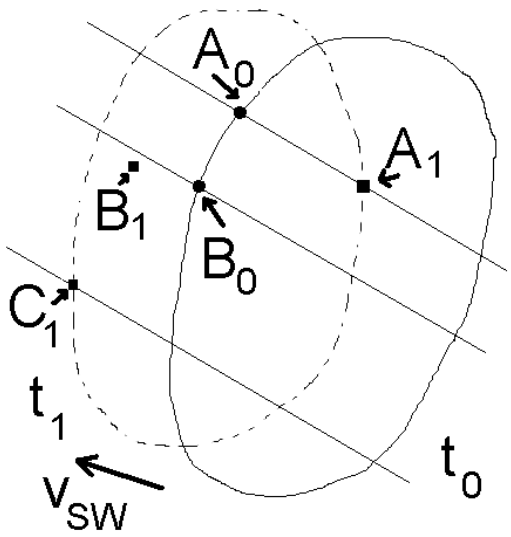

Figure 4: *Two methods for HFA size estimation. A_0, A_1: estimation with one spacecraft. B_0, B_1 and C_1: estimation method with two spacecraft.*

parallel with the x axis of the simulation box. A tangential discontinuity is generated in the flow after forming bow shock. The angle between the normal vector of the tangential discontinuity and the direction of the flow might be variable. Simulations with different angles were performed. The results predict that the size of HFAs are of the order of 1-3 Earth radii. The form of the profiles look alike in the first simulation, however, the temperature increases to a value 100 times higher, the solar wind speed decreases to 50-80%. The density of the solar wind decreases to 55-75% in the middle of the event but increases to 140% at the rim.

3.2 Comparison with observations

Analyzing fifty HFA events we can say that the shape of the temperature, the density and the magnitude of the magnetic field profiles qualitatively agree with the results of simulations. The quantitative result is not so close, however, these simulations were performed for idealistic and very simple cases thus we must not expect a better accordance. The simulations also describe well the attendance and development of HFAs.

We used two different methods to estimate the size of HFAs (See Fig. 4). The

spacecraft enters into the HFA in A_0 at t_0 and leaves it in A_1 at t_1. The HFA is traveling with the solar wind till the satellite is flying inside of the structure thus we get the distance from the $d = v_{SW} \cdot (t_1 - t_0)$ equation. We might neglect the speed of the satellite because $v_{s/c} \ll v_{SW}$. This is not very accurate because the solar wind speed might change and the HFA is not frozen into the plasma of the solar wind. So we have used another multispacecraft method, too (See Fig. 4). The B spacecraft intersects the border of HFA in B_0 at t_0. The C spacecraft do the same in C_1 at t_1. However, the position of the HFA changes until the second (C) satellite intersects its border. We can calculate the new position of the B_0 point from the position of the B_0 and the speed of the solar wind using the $\overrightarrow{r}_{B_1} = \overrightarrow{r}_{B_0} + \overrightarrow{v}_{SW} \cdot (t_1 - t_0)$. The HFA size must be larger than the distance between B_1 and C_1. We calculate this distance from the coordinates. If more then two spacecraft detect the same HFA then we can calculate all distances and use the longest.

We obtained very exciting result after determining the size of the HFA events. The size of the affected region seems to be 2-10 Earth radii with the first method based upon the time of pass. If at least two spacecraft cross HFA we could estimate the minimal diameter of the event. This second method gave values of 0.65-2.2 Earth radii. Both results are in agreement with the forecast of the simulations. Actually the first method based upon the time of cross doesn't seem to be accurate. Its error larger then the second method thus it is more practical to use this method if it is possible.

4 Summary

We set up conditions for HFA events and processed the mesurements of CLUSTER RAPID, FGM and CIS instruments between February and April, 2003. We found about fifty new events and developed a method for calculating transformed pitch angle distributions taking the Compton-Getting effect into account. We demonstrated our method by calculating of two kinds of PADs for the same HFA event. We also estimated the size of HFAs and compared with observations and found agreement with predicted values.

The second simulation (Lin, 2002) with different angles between the tangential discontinuity and the direction of the flow indicated that the size depends on this angle (γ). Higher γ values result in larger HFA up to about 80^o. If γ is greater than 80^o, the size decreases. The size of HFA also depends on the directional change of the magnetic field *before* and *after* the tangential discontinuity ($\Delta\Phi$). Unfortunately it seems to be very difficult to determine the values of these γ and $\Delta\Phi$ angles, so this problem needs to be solved in the future.

A new research area was created when Mars Global Surveyor discovered HFA events around Mars (Øieroset, 2001). This fact might be the first proof of that HFAs are general phenomena. HFAs might appear where bow shock and tangential discon-

tinuity interacts: around Jupiter, Saturn, ahead of CME[6]s, at the heliopause, or in interstellar clouds as well. The solution of this problem deserves further experimental and theoretial research.

Acknowledgement

The authors thank the OTKA grant T037844 of the Hungarian Scientific Research Fund for support.

References

Compton, H., Getting, I. 1935, Phys. Rev. E, 47(11), 817

Escoubet, C. P., Russell, C. T., Schmidt, R. (eds.) 1997, The Cluster and Phoenix Missions, Kluwer Academic Publishers

Facsko, G., 2004, Publications of the Astronomy Department of the Eötvös Lóránd University, Vol. 14, p. 25-33

Lin, Y., 1997, J. Geophys. Res., Vol. 102, NO. A11, p. 24265-24281

Lin, Y., 2002, Planet. Space Sci., 50, p. 577-591

Lin, Y., 2003, J. Geophys. Res., Vol. 108, NO. A11, 1390, doi:10.1029/2003JA009991

Lucek, E. A., Horbury, T. S., Balogh, A., Dandouras, I., Rme, H., 2004, J. Geophys. Res., Vol. 109, A06207, doi:10.1029/2003JA010016.

Øieroset, M., Mitchell, D. L., Phan, T. D., Lin, R. P., Acuña, M. H., Geophys. Res. Lett., 2001, Vol. 28, NO. 5., p. 887-890

Schwartz, S. J., Chaloner, C. P., Christiansen, P. J., Coates, A. J., Hall, D. S., Johnstone, A. D., Gough, M. P., Norris, A. J., Rijnbeek, R. J., Southwood, D. J., Woolliscroft, L. J. C., 1985, Nature, Vol. 318, p. 269-271

Schwartz, S. J., Paschmann, G., Sckopke, N., Bauer, T. M., Dunlop, M., Fazakerley, A. N., Thomsen, M. F., 2000, J. Geophys. Res., Vol. 105, NO. A6, p. 12639-12650

Sibeck, D. G., Borodkova, N. L., Schwartz, S. J., Owen, C. J., Kessel, R., Kokubun, S., Lepping, R. P., Lin, R., Liou, K., Lühr, H., McEntire, R. W., Meng, C.-I., Mukai, T., Nemecek, Z., Parks, G., Phan, T. D., Romanov, S. A., Safrankova, J., Sauvaud, J.-A., Singer, H. J., Solovyev, S. I., Szabo, A., Takahashi, K., Williams, D. J., Yumoto, K., Zastenker, G. N., 1999, J. Geophys. Res., Vol. 104, NO. A3, p4577-4594

Thomas, V. A., Wiske, D., Thomsen, M. F., Onsager, T. G., 1991, J. Geophys. Res., Vol. 96., NO. A7, p. 11625-11632

[6]**C**oronal **M**ass **E**jection

Thomsen, M. F., Gosling, J. T., Fuselier, S. A., Bame, S. J., Russell, C. T., 1986, J. Geophys. Res., Vol. 91, NO 10., p11311-11325